Basic flow processes in high pressure fuel injection equipment

Ernst Winklhofer[1], Erich Kelz[2], Alexander Morozov[3]

1. AVL List GmbH, Graz, Austria
2. University of Technology, Graz, Austria
3. University of Technology, Graz, Austria

Fuel injection systems (FIS) for diesel engines aim at ever higher injection pressures as this has proven to effectively support emissions reduction strategies. Part of manufacturing FIS components for best practical use requires the thorough understanding of fuel flow behaviour and how the injection and spray formation process can be influenced by FIS design parameters and operating modes. Fuel flow into and through the nozzle holes is understood to be of central importance for best system quality.
The trend towards ever higher injection pressures is accompanied by ever smaller nozzle hole cross sections. This results in growing influence and practical importance of nozzle hole geometry, both on the macroscopic scale as defined by nozzle hole length, diameter, hole conicity and inlet or outlet radius, but also by microscopic geometry given by the roughness of the nozzle hole surface.
The paper describes experiments which were designed to allow optical inspection and measurement of local fluid flow conditions under the influence of macroscopic and microscopic geometry variations. The focus of this experimental study was put into the realisation of fluid flow conditions which are expected to be representative for flow situations in high pressure FIS, and the set-up should simultaneously allow the thorough measurement of flow properties such as local pressure, velocity, and liquid - vapour phase probability. This request for comprehensive flow measurements resulted in the design of optically accessed model flow components which are well defined with respect to their boundary and operating conditions, but they were not designed to follow any overall similarity considerations with real FIS components.

1. Experimental arrangements

Parts of the experimental set-up for this work have been described in earlier publications, see [1] and [2]. The following describes the experimental set-up and measurement techniques as required to understand the results of this study.

1.1 The 2-D model flow rig

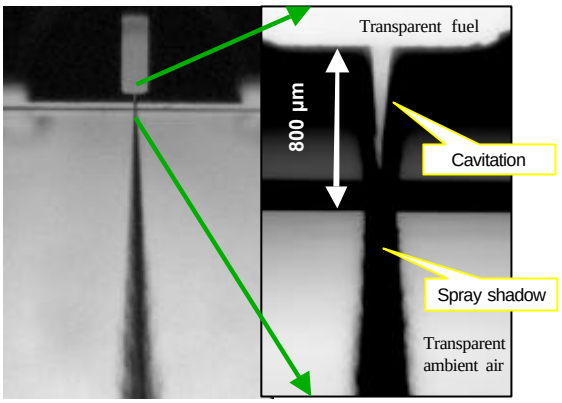

Fig. 1a The model nozzle arrangement with the free spray

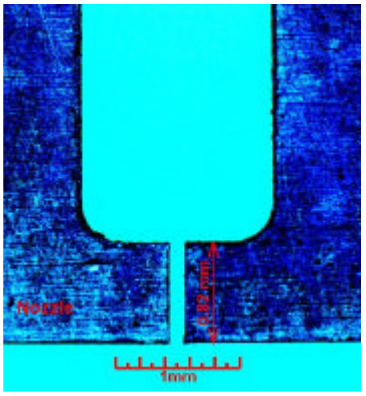

Rectangular nozzle in steel sheet:
820 µm long, 110 µm wide, 100 µm thick

Fig. 1b Nozzle geometry details

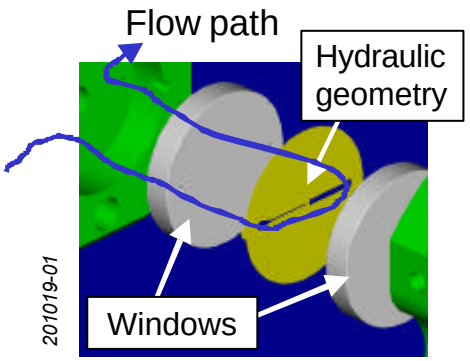

Fig. 1c The model throttle flow path between the sapphire windows

The flow geometry of interest is eroded into steel sheets. The sheets are sandwiched between a pair of sapphire windows. The low pressure side is either open to ambient air for nozzle flow and free spray studies, see Fig. 1, or it is a liquid volume which is pressurised for throttle flow studies, as shown in the design sketch of Fig. 1C. The hydraulic components comprise a fuel tank, fuel supply pump, high pressure common rail pump, pressure regulator, inlet valve, the optically accessed 2-D flow model, and a free test section in ambient air for spray experiments, or outlet valves and return line for throttle flow studies. One set of experiments was made with injecting into a pressurised chamber with compressed air or fuel, respectively. Fuel pressure levels are measured 35 mm upstream and downstream (if applicable) of the observation element (DMS sensor, AVL SL31D200). For stationary conditions, fuel mass flow is measured with a coriolis sensor (Danfoss, Mass 2100 sensor and Mass 3000 signal converter).

1.2 Visualisation of cavitation field

This is accomplished by back illumination and imaging of the flow model with a CCD camera (100 ns illumination time). The gas bubbles created in the low pressure cavitation areas result in the blackening of the observed flow area. This is directly recorded on a CCD camera. As cavitation bubbles are created in a highly turbulent flow environment, the location of the cavitation field is fluctuating. Local fluctuation probability is visualised by means of distribution pattern statistics. This is based on binarisation of the grey scale images and subsequent ensemble averaging for a set of 20 images taken under the same operating conditions. Results are then presented as probability distribution fields of the local light transmittance (see e. g. Fig 2).

1.3 Visualisation of the pressure field

The basis of the pressure field visualisation is the measurement of the optical path length field in the 2-D model flow. For this purpose a Mach Zehnder interferometer arrangement is used. The interferograms are recorded with a CCD camera at 500 ns recording time. The interferogram fringe shift evaluation is based on an FFT algorithm [2]. Results are ensemble averaged for 20 images per operating condition. The optical path length data in the 2-D geometry are converted to density data and density to pressure and temperature data. For constant fluid temperature, this evaluation yields the pressure field. However, as heat is generated in the flow by turbulent dissipation, an error introduced by temperature rise must be accounted for. This temperature rise across the throttle was between 2 and 3 K. With the given arrangement, the error by neglecting this temperature effect is below 3% of the locally determined pressure level [1].

1.4 Velocity profiles

Velocity profiles are measured with a fluorescence tracing method. A narrow area of the fluid is irradiated with a laser light pulse (248 nm, 30 ns). This area is precisely located by means of a reference image. The irradiation yields fluorescence emission of the diesel fluid. An image of the fluid, captured at a constant time interval after the illumination with the laser pulse shows the displacement of the irradiated flow area during this time interval.
This displacement against the reference image together with the selected time delay directly yields the velocity profile.

1.5 Hydraulic measurements

Mass flow versus pressure drop measurements were made to find the individual throttles' transition into choked flow conditions. This procedure was standardised for an inlet pressure of 100 bar (above ambient) and a fuel inlet temperature of 27 deg C. The mass flow first follows the rising pressure drop as outlet pressure is decreased from near 100 bar to ambient pressure. With the onset and growth of cavitation, however, the massflow approaches a constant level and is insensitive to further reduction of outlet pressure. This transition from pressure dependent mass flow to choked mass flow defines the "critical cavitation" (CC) point. For practical purposes, the critical cavitation pressure (CCP) is defined as the pressure drop where the mass flow along the hydraulic line approaches 99% of the choked mass flow.

With the widely used definition of the cavitation number

$$CN = (P_{in} - P_{out}) / (P_{out} - P_{vapor}) \quad (1)$$

the critical cavitation number is defined as

$$CCN = CCP / (P_{out\ at\ CCP} - P_{vapor}) \quad (2)$$

P_{vapor} for diesel fuel at 31 deg C is 20 mbar.

If inlet pressure is maintained at 100 bar and constant temperature, CCN for a given liquid is only dependent on throttle geometry. For further details see refs. [1] and [2].

2. Scope of results

The results section of this paper starts with a demonstration of nozzle flow and spray modes. It is understood that at sufficiently high pressure drop, the flow through the nozzle is cavitating. This requires the local pressure to drop below vapour pressure and thus raises the interest for pressure field distribution inside the nozzle. Consequently, flow velocities come into the interest, both inside the nozzle, as well as in the free spray. As nozzle geometry is a design parameter for hydraulic flow engineering, the influence of macroscopic dimensions such as sharp and smooth inlet curvatures as well as the influence of surface irregularities (roughness) on cavitation are tested.

3. Nozzle flow and spray modes

Raising the inlet pressure in a transient flow experiment first yields a laminar, straight jet which, at increasing pressure drop, transits into a turbulent spray with an apparently larger macroscopic spray cone angle. As the spray cone angle is accessible for systematic studies also in unmodified spray experiments, there is vast literature to describe spray cone and spray core trends in response to injection system parameters [3,4]. The view into the model nozzle hole in Figs. 2 and 3 shows the transition from liquid phase nozzle flow at low pressures to cavitating flow at pressures above 210 - 290 bar. The characteristics of this cavitating nozzle flow in the 2D arrangement of our experiment are the cavitation downstream of the nozzle inlet and the central liquid core at the inlet. In the actual experiment this internal nozzle flow pattern is fully established at pressures above 290 bar, see the summary in the transient pressure chart of Fig. 4.
The internal nozzle flow pattern with the liquid core surrounded by cavitation layers pertains as inlet pressure is raised up to 1100 bar. The only noticeable variation is the shortening of the

central liquid core, see Fig. 3. Similar experiments have been reported from transparent 3D nozzle experiments [4,5].

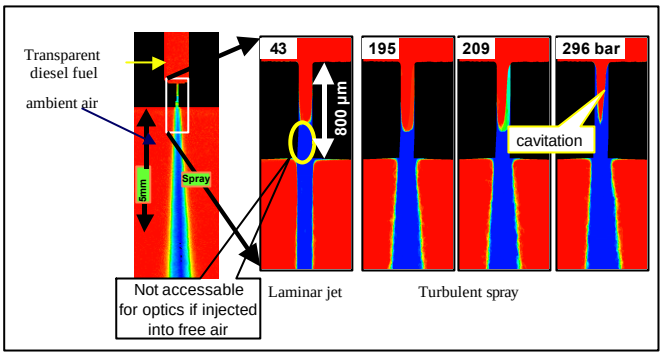

Fig. 2 Rising inlet pressure first yields a laminar jet, then a turbulent spray and finally a cavitating turbulent spray

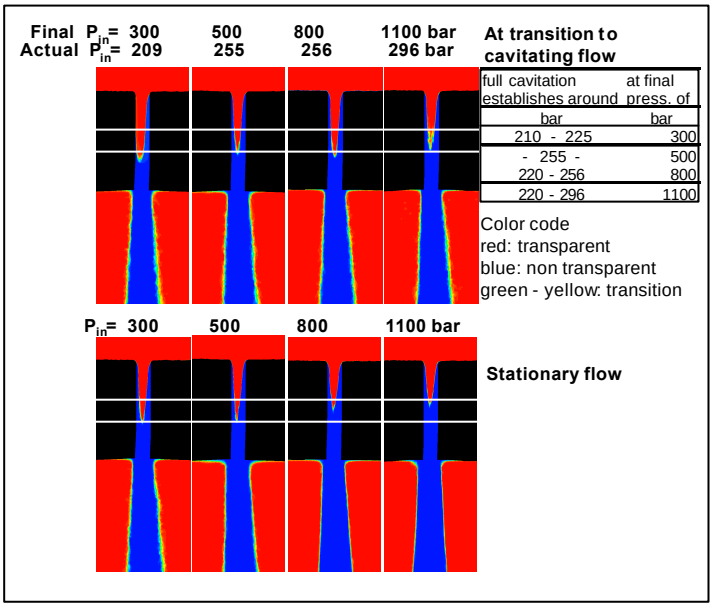

Fig. 3 Cavitating turbulent spray with cavitation at the nozzle inlet extending towards the nozzle hole exit and a liquid core in the central nozzle hole entrance area

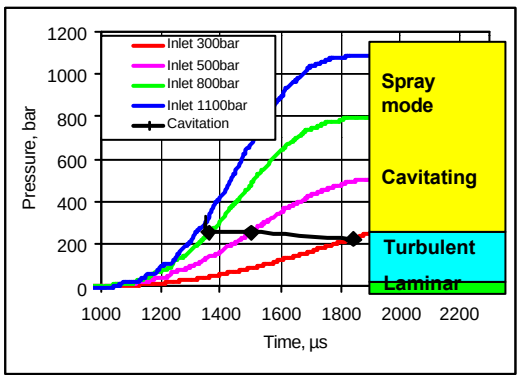

Fig. 4 Pressure chart shows transition from turbulent into fully cavitating spray mode

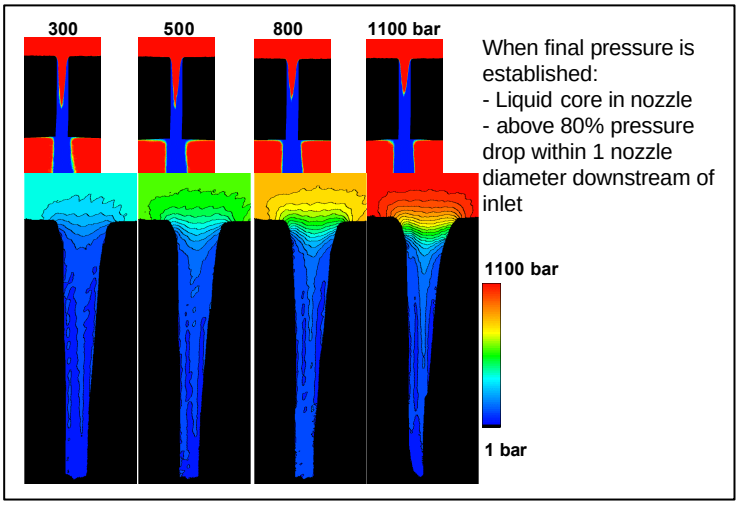

Fig. 5 Pressure distribution in liquid core at nozzle entrance

The pressure drop within the liquid core is shown in Fig. 5. The interferometric measurements show that the main part of the inlet pressure is already converted within about 1 nozzle diameter downstream of the geometric entrance. The structure of the pressure field, furthermore, is rather independent of the overall pressure.

The velocity profile of the liquid core is quite uniform across the diameter, see Fig. 6. Velocities of the free spray are given in Fig. 7. The profiles are essentially flat across the spray (see also [6]) and they drop at the spray periphery. The velocity and pressure field data are compared with Bernoulli estimates of the pressure drop to velocity conversion. For the cross section M1 inside the nozzle and for the free spray velocities at the position 5 mm downstream of the orifice, the data are summarised in Table 1. The actually measured velocities, both inside the nozzle hole, as well as in the free spray are consistently about 10% below the Bernoulli estimate.

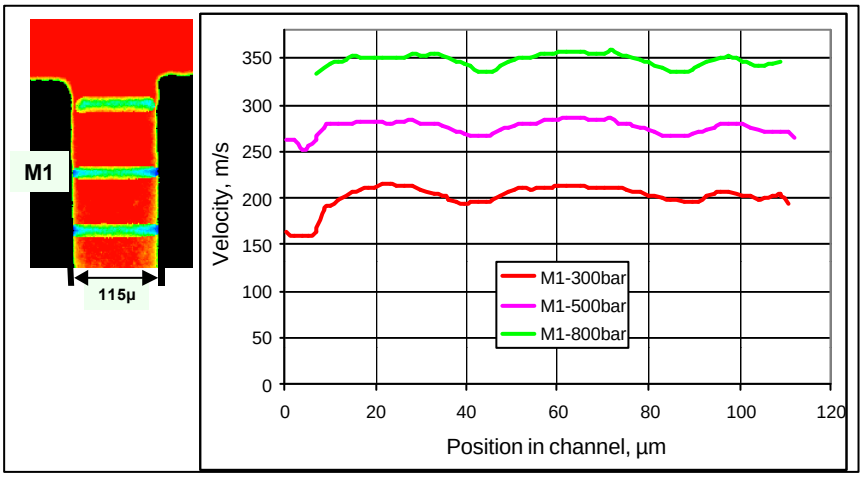

Fig. 6 Velocity profiles inside the rectangular spray hole

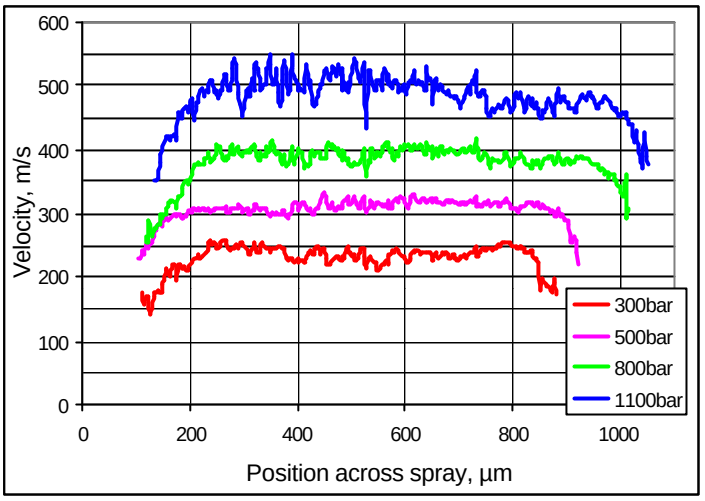

Fig. 7 Velocity profiles in the free spray

Table 1. Velocity measurements in nozzle flow and spray. Comparison with Bernoulli velocities

P_{inj}, bar	**$V_{Bernoulli}$** Flow-M1 m/s	**V_{LIF}** Flow-M1 m/s	**V_{LIF}/V_{Bern} Flow-M1**	**$V_{Bernoulli}$** Spray m/s	**V_{LIF}** Spray at 5mm m/s	**V_{LIF}/V_{Bern} Spray**
300	239	215	**0.90**	267	239	**0.89**
500	309	282	**0.91**	345	312	**0.91**
800	390	355	**0.91**	436	392	**0.90**
1100	-	-	**-**	512	488	**0.95**

The Bernoulli velocity is calculated from the pressure drop ΔP and the fluid density (840 kg/m³ for diesel fuel of this experiment)

$$V_{Bern}(m/s) = \sqrt{\frac{2 \cdot \Delta P(bar) \cdot 10^5}{840}} \qquad (3)$$

Local pressure levels were obtained from the interferometry measurements. For the position M1 the actual pressure drop is approximately $\ddot{A}P_{M1}=0.8\ P_{inj.}$

4. Phenomena analysis

Following the above overview of nozzle and spray flow properties, focus was given into the further analysis of

- back pressure influence on internal nozzle flow
- injection into gas (nozzle flow) versus injection into liquid (throttle flow)
- cavitation formation: where does it appear, how can cavitation regimes grow
- geometry influence on incipient cavitation: macroscopic and microscopic effects

4.1 Back pressure influence

Injecting into pressurised gas atmosphere requires higher inlet pressures to establish fully cavitating nozzle flow. The nozzle flow patterns of Fig. 8 show the formation of cavitation regimes in the flow separation areas at the inlet throat. Downstream of the entrance contraction, however, the full liquid flow is re-established and again attaches to the nozzle wall. For the actual nozzle geometry, it requires inlet pressures above 300 bar to generate full cavitation along the nozzle hole if back pressure is 50 bar, see Fig. 8. Fig. 9 gives a comparison of stationary flow patterns at various constant inlet and outlet pressure combinations.

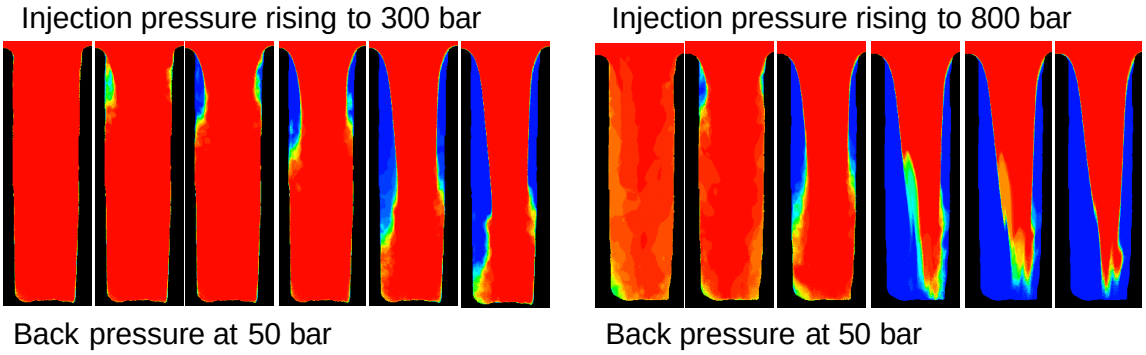

Fig. 8 Internal nozzle flow patterns as inlet pressure rises to 300 and 800 bar, respectively

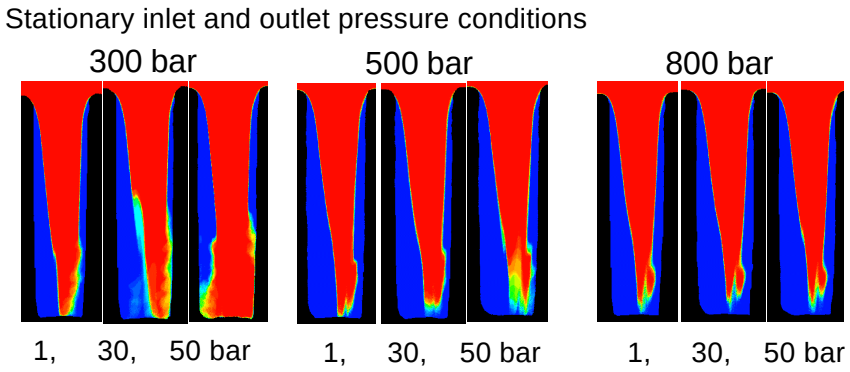

Fig. 9 Nozzle flow patterns at stationary inlet and outlet pressure conditions

4.2 Injection into gas versus injection into liquid

Experiments were also done with injection into liquid rather than gas. The results show that the flow inside the nozzle hole, once full cavitation is established, and especially under stationary conditions, has no apparent difference. There is of course different behaviour under transient conditions, as downstream liquid has to be accelerated and generates dynamic back pressure for the upstream flow. At stationary conditions flow patterns are practically identical, see the example in Fig. 10.

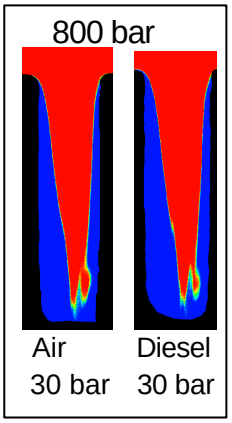

Fig. 10 Injection into gas and liquid. Under cavitation conditions no apparent difference of internal nozzle flow pattern

As a consequence of the independence of the downstream medium on cavitating stationary nozzle flow, nozzle hole cavitation studies (liquid into gas) and throttle hole cavitation studies (liquid into liquid) are equivalent as far as they are confined to the regime upstream of the exit orifice plane.

This equivalence makes it possible to discuss a large number of cavitation effect, especially those which are relevant for throttle or nozzle inlet flow on the same basis. Cavitation formation, inlet geometry effects and boundary layer phenomena are typical examples.

4.3 Cavitation formation: where does it appear, how can cavitation regimes grow

Throttle cavitation studies have in detail been presented in [1] and [7]. These papers cover overall hydraulic flow assessment as well as local flow field data for pressure and velocities. Cavitation formation at inlet contractions was essentially identified as the result of local shear flow effects - i. e. flow velocity profiles - under the influence of and interaction with local static pressure conditions. Both were found to be the result of the overall pressure and geometry conditions for the given flow medium (and temperature). The "critical cavitation number" CCN which in practical applications is used to describe the cavitation property of a specific throttle arrangement was found to be linked to the transition from partial to full cavitation inside the throttle orifice [7] .

4.4 Geometry influence on incipient cavitation: macroscopic and microscopic effects

The study in [1] has shown that cavitation at the inlet contraction into a throttle hole for nominally identical macroscopic inflow geometry occurs at nearly identical overall flow velocities or massflows. Macroscopic geometry and massflow, thus result in identical local conditions for cavitation, see also Table 2.

A large inlet radius (throttle YL) considerably raises CCN, as cavitation requires higher pressure drop to be established. The roughening of the throttle surface, however, decreases CCN (throttle YR).

Table 2 J, U, W data from [1] with corrected and updated velocities. YR: rough surface, YL: smooth surface. For all throttles: 301 µm thick steel sheet, sharp outlet, 1 mm throttle length, 100 bar inlet pressure.

Throttle	Inlet	Inlet	Outlet	Contraction	**Hydraulic data at cavitation start CS**				**Hydraulic data at critical cavitation CC**			
	radius	width	width									
	R1	D1	D2		Äp	mass fl.	CN	v	Äp	mass fl.	CCN	v
	µm	µm	µm	%	[bar]	[g/s]		[m/s]	[bar]	[g/s]		[m/s]
J	20	299	299	0	57.0	7.21	1.33	110	65.0	7.72	1.86	124
U	20	301	284	5	60.0	7.17	1.50	109	70.0	7.74	2.33	123
W	20	301	270	10	67.0	7.17	2.03	112	77.0	7.76	3.35	135
YL	100	299	299	0	84	9.07	5.26	117	87.0	9.55	6.70	120
YR	100	312	312	0	68	8.65	2.13	115	76.0	9.45	3.17	127

The hydraulic data, the flow field analysis and the comparison of the smooth and rough throttle (YL and YR) details are given in Fig. 11 to 15. Observe that the YR throttle is 13 µm wider than the YL throttle!

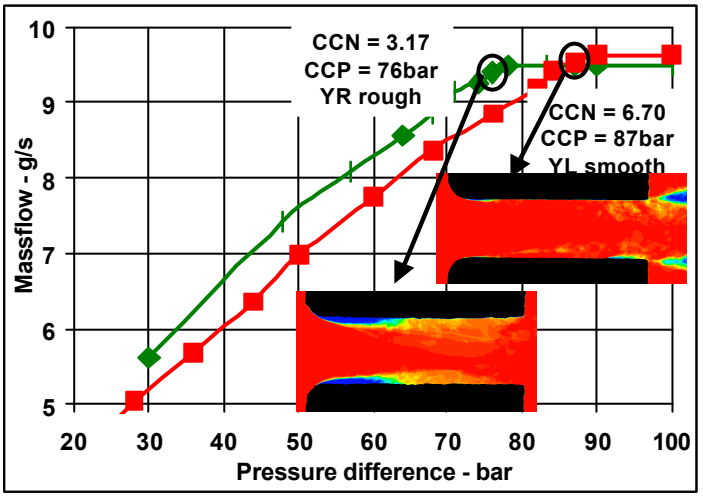

Fig. 11 Hydraulic data of YL and YR throttle. Notice that YR throttle is 13 µm wider

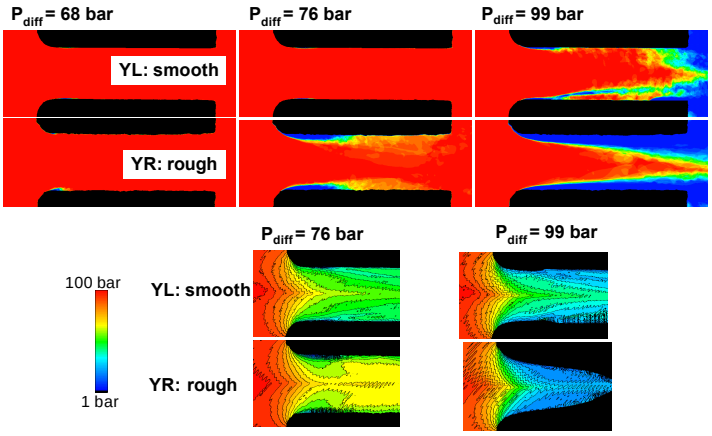

Fig. 12 Cavitation field and pressure field of YL and YR throttle

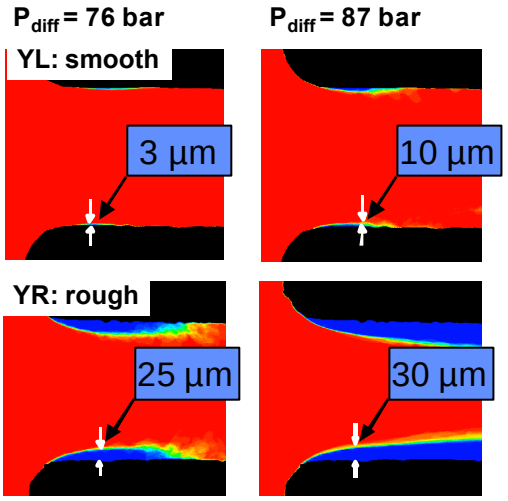

Fig. 13 Cavitation boundary layers for smooth and rough inflow

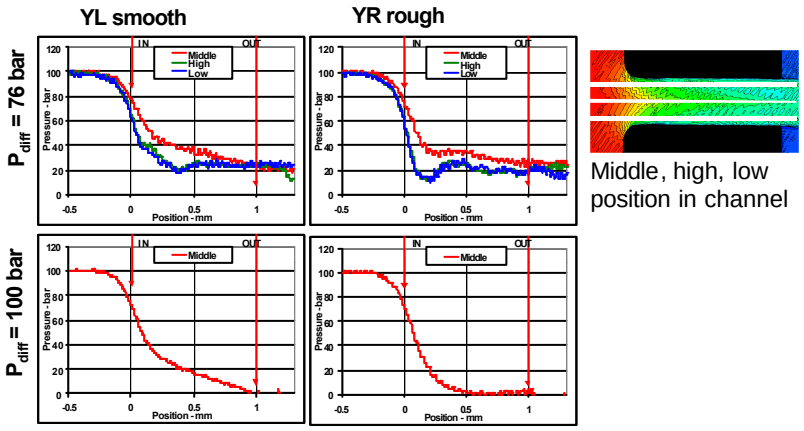

Fig. 14 Comparison of pressure profiles along control lines

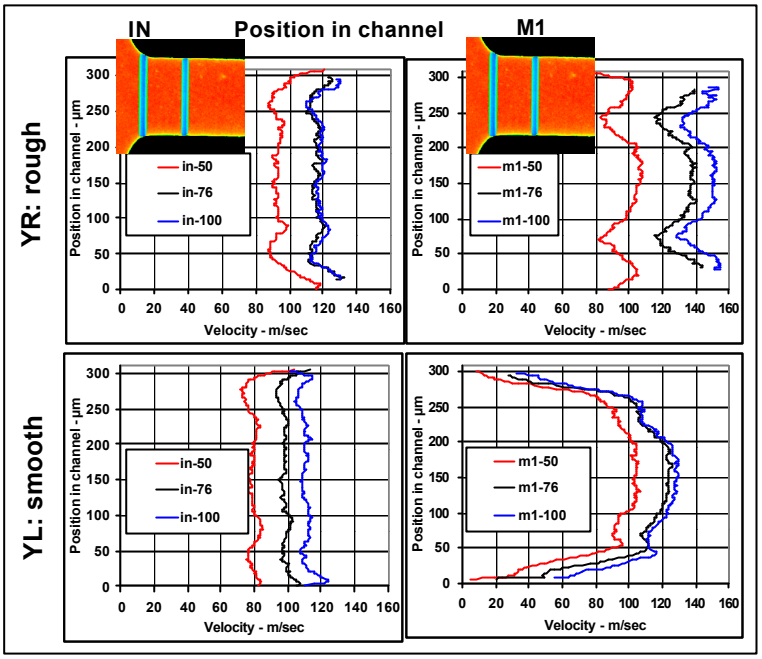

Fig. 15 Velocity profiles in flow channel for smooth and rough surface throttle

The overall comparison shows that the rough surface in the YR throttle generates the usual cavitation layer in the flow separation regime at the throttle entrance. At increasing pressure drop these cavitation areas increase in a similar way as is also found in sharp edged throttle inlets [1]. Without the roughening, the inlet flow into throttle YL just forms very small cavitation layers. Even at the maximum pressure drop of this experiment, at 100 bar inlet against 1 bar outlet pressure, the throttle hole still is mainly filled with transparent liquid, rather than cavitation bubbles. Cavitation, however occurs across the entire cross section of the exit orifice.

Enlarged photographs of the throttle inlet show the growth of the cavitation layers in both the rough and the smooth throttle, Fig. 13. Cavitation bubbles in the rough throttle are generated downstream of surface irregularities. They are then convected into the entrance flow contraction, where they can cover an ever growing area as pressure drop is increased (outlet pressure is decreased). Under the same overall conditions, the smooth surface of throttle YL does not provide the irregularities to generate sufficient cavitation sources at the entrance contraction. The cavitation layers in the inlet flow contraction stay small even as downstream pressure is decreased to ambient.

The pressure field comparison in Fig. 12 shows the consequence of this cavitation layer mechanism with respect to the entire flow cross section. With the flow separation and cavitation layer build-up at the rough throttle, the pressure near the wall first drops and then recovers again before full cavitation is established. With the smooth surface throttle, the pressure drop is confined to a very narrow layer at the throttle wall. This overall trend is further shown with the pressure profile data along the throttle centre and along boundary lines, see Fig. 14.

The velocity profiles of these flow situations are given in Fig. 15 for 50, 76 and 100 bar pressure drop for the cross sections "IN" and "M1" near the throttle inlet, see positions in the figure insert. In the inlet cross section IN, velocity profiles of both the rough and smooth

throttle show a turbulent profile across the main part of the throttle channel. Near the wall, there is the typical velocity increase due to the incipient cavitation (gas) boundary layer in the rough throttle. This increased velocity layer extends for about 30 µm on either side of the YR throttle. With the smooth throttle, this high velocity boundary layer is considerably smaller (10 to 20µm at most), and within a 5 µm layer near the wall, there is even velocity drop discernible.

At the downstream cross section M1, the velocity profiles have considerably changed. With the rough surface throttle YR, the cavitation near the wall allows the velocity profiles to peak as laminar liquid surface layers do not exist. In contrast, the smooth surface throttle YL shows that the velocity profiles drop significantly within a boundary layer of around 40 µm from about 100 m/s to near zero.

5. Summary

High pressure fuel injection events have been studied in a transparent model nozzle and model throttle, respectively. A 2-D experimental arrangement provided the optical access for the comprehensive study of the pressure-, velocity- and cavitation fields generated by the flow through the nozzle or throttle orifice.
Nozzle experiments have shown that the high pressure flow through the model nozzle hole is always governed by cavitation. As full cavitation at the nozzle hole entrance is established at around 250 bar, a highly stabilised flow pattern comprising a central liquid core in the entrance to the nozzle hole and surrounding cavitation areas is maintained even as inlet pressure is increased up to 1100 bar.
Backpressure at the nozzle exit requires higher inlet pressure to establish full cavitation.
Injection into liquid rather than gas has no noticeable influence on the flow, once full cavitation is established. It has, however, influence under transient conditions as it requires acceleration and deceleration of the fluid.
Cavitation was always found to be governed by the macroscopic flow (pressure drop and flow geometry) which allows low pressure areas to be established together with high shear force flow regimes.
Incipient cavitation was found to originate in shear layers, either within the flow, or at wall boundary layers. Wall boundary layers are susceptible to surface irregularities, and, consequently, rough surfaces near low pressure flow areas are acting as triggers for microscopic flow separation and ensuing formation of cavitation layers. Via interaction with the overall flow, these microscopic irregularities can initiate large scale flow effects in the downstream flow field. Examples have been given for a rounded inlet throttle with smooth and rough surfaces.

References

[1] E. Winklhofer, E. Kull, E. Kelz, A. Morozov: *Comprehensive hydraulic and flow field documentation in model throttle experiments under cavitation conditions* (ILASS Europe 2001, Zürich, Sept. 2001)

[2] E. Winklhofer, H. Philipp, A. Hirsch, A. Morozov: *Cavitation and spray formation in diesel flow situations* (ILASS Europe 2000, Darmstadt 11-13 September 2000)

[3] H. Hiroyasou, M. Arai: *Structure of fuel sprays in diesel engines* (SAE 900475)

[4] V. Schwarz, G. König, M. Blessing, C. Krüger, U. Michels: *Einfluss von Strömungs- und Kavitationsvorgängen in Dieseleinspritzdüsen auf Strahlausbreitung, Gemischbildung, Verbrennung und Schadstoffbildung bei HD-Dieselmotoren* (Berichte zur Energie- und Verfahrenstechnik, ISBN 3-931901-27-0, Erlangen, 2003)

[5] H. Chaves, M. Knapp, A. Kubitzek, F. Obermeier, T. Schneider: *Experimental study of cavitation in the nozzle hole of diesel injectors using transparent nozzles.* (SAE 950290)

[6] C. Schugger, U. Renz: *Experimental investigation of the primary breakup of high pressure diesel sprays* (ILASS Europe 2001, Zurich 2-6 Sept. 2001)

[7] E. Kull, E. Winklhofer: *Einfluss der Geometrie eines Spritzlochmodells auf Kavitation und Massenstrom* (Berichte zur Energie- und Verfahrenstechnik, ISBN 3-931901-27-0, Erlangen, 2003)